Preantral follicular atresia occurs mainly through autophagy, while antral follicles degenerate mostly through apoptosis

Meng, L., Jan, S. Z., Hamer, G., van Pelt, A. M., van der Stelt, I., Keijer, J., & Teerds, K. J.

Preantral follicular atresia occurs mainly through autophagy, while antral follicles degenerate mostly through apoptosis

Running title: Autophagy, apoptosis and follicular atresia

Summary sentence: Preantral and antral follicles make use of different cell death pathways, as antral follicular degeneration is initiated by massive granulosa cell apoptosis, while preantral follicular atresia is mainly dependent on enhanced granulosa cell autophagy

Key words: Apoptosis, autophagy, atresia, preantral and antral follicles, granulosa cells, mitochondria, ovary

Li Meng[a,b], Sabrina Z. Jan [c], Geert Hamer[c], Ans M. van Pelt[c], Inge van der Stelt[a], Jaap Keijer[a], Katja J. Teerds[a]*

[a]Human and Animal Physiology, Wageningen University, P.O. Box 338, 6700 AH, Wageningen, The Netherlands

[b]National Engineering Research Center For Breeding Swine Industry, College of Animal Science, South China Agricultural University, Guangzhou, Guangdong 510642, P.R. China

[c]Reproductive Biology Laboratory, Academic Medical Center, University of Amsterdam, Q3.119, Meibergdreef 9, 1105 AZ, Amsterdam, the Netherlands

Footnote 1:

Li Meng was funded by the China Scholarship Council (CSC) under grant number 2011685003.

Footnote 2:

Corresponding author: Katja Teerds, PhD

Human and Animal Physiology

Department of Animal Sciences, Wageningen University

P.O. Box 338, 6700 AH, Wageningen, The Netherlands

Tel.: +31-317-483014

E-mail: katja.teerds@wur.nl

Abstract

There is general agreement that granulosa cell apoptosis is the cause of antral follicle attrition. Less clear is whether this pathway is also activated in case of preantral follicle degeneration, as several reports mention that the incidence of granulosa cell apoptosis in preantral follicles is negligible. Our objective is therefore to determine which cell-death pathways are involved in preantral and antral follicular degeneration.

Atretic preantal and antral follicles were investigated using immunohistochemistry and laser-capture micro-dissection followed by qRT-PCR. Microtubule-associated light-chain protein 3 (LC3), sequestosome 1 (SQSTM1/P62), Beclin1, autophagy-related protein 7 (ATG7) and cleaved caspase 3 (cCASP3) were used as markers for autophagy and apoptosis, respectively. P62 immunostaining was far less intense in granulosa cells of atretic compared to healthy preantral follicles, while no difference in LC3 and BECLIN1 immunostaining intensity was observed. This difference in P62 immunostaining was not observed in atretic antral follicles. mRNA levels of LC3 and p62 were not different between healthy and atretic (pre)antral follicles. ATG7 immunostaining was observed in granulosa cells of preantral atretic follicles, not in granulosa cells of degenerating antral follicles. The number of cCASP3 positive cells was negligible in preantral atretic follicles, while numerous in atretic antral follicles. Taken together, we conclude that preantral and antral follicular atresia is the result of activation of different cell-death pathways as antral follicular degeneration is initiated by massive granulosa cell apoptosis, while preantral follicular atresia occurs mainly via enhanced granulosa cell autophagy.

Introduction

The most important functions of the female gonad are the formation and release of mature oocytes and the production of steroids necessary for the development of female secondary sexual characteristics. From the pool of dormant primordial follicles, follicles are continuously recruited into the pool of growing follicles, a process that takes place independent of gonadotropic hormones. These follicles grow until the early antral stage; estrous cycle dependent increases in circulating follicle-stimulating hormone (FSH) concentrations are responsible for the cyclic recruitment of a cohort of small antral follicles, from which the dominant follicles are selected [1]. Follicular development is not a very efficient process as over 99% of ovarian follicles degenerate before ovulation by a process named atresia. In the adult female, atresia ensures that only healthy follicles, containing oocytes of optimal quality, will ovulate [1, 2]. Although follicular atresia affects all stages of follicular development, the highest incidence of follicular degeneration is observed when follicles become dependent on FSH, at the early antral follicle stage. Preantral and preovulatory follicles rarely undergo atresia [3].

It has long been assumed that granulosa cell death by apoptosis is the main cause of follicular atresia [4]. Recently, it has become increasingly apparent that apoptosis may not be the only process involved in follicular degeneration, but that other forms of cell death, such as autophagy, may also participate in this process. Hulas-Stasiak and Gawron [5] have shown that in the neonatal period when primordial and primary follicles undergo massive degeneration, autophagy is the dominant form of follicular atresia. Another study reported that human granulosa cells exposed *in vitro* to oxidized low-density lipoprotein show morphological signs of autophagy [6], while Choi et al. [7] have demonstrated the presence of microtubule-associated light-chain protein 3 (LC3), a marker for autophagy, in the rat ovary.

Autophagy is an evolutionary conserved intracellular mechanism whereby damaged organelles and proteins are degraded, recycled and prepared for reuse by the cell. Three types of autophagy can be distinguished in mammalian cells: chaperone-mediated autophagy, micro-autophagy and macro-autophagy. Macro-autophagy (herein referred to as autophagy) constitutively occurs at a low level in cells, but can be further induced by stressful conditions such as nutrient or energy starvation,

accumulation of reactive oxygen species (ROS) or infection [8]. Autophagy functions primarily as a cytoprotective mechanism. However, autophagic dysfunction due to excessive self-degradation can lead to a number of pathologies, including neurodegeneration, cancer and metabolic diseases [9]. Autophagy is a multistep process that involves the activation of a complex molecular machinery. LC3 is an important protein involved in autophagy, as it determines the size of the autophagosome, participates in cargo recognition and is therefore widely used as marker to monitor autophagy [10]. LC3 is synthesized in an inactive form, pro-LC3, that immediately after synthesis is processed to generate soluble LC3-I, which can be converted into an active autophagosome membrane-bound form, LC3-II [10]. Autophagy-related protein 7 (ATG7) is essential for the assembly and function of LC3 in the expansion of autophagosomal membranes, and therefore considered to be of the utmost importance in autophagy-related cell homeostasis. ATG7 can thus be regarded as an early marker of autophagy [reviewed in 11].

Ubiquitin-binding protein sequestosome 1 (SQSTM1/P62, further named P62) plays an important role in the clearance of ubiquitinated protein aggregates by functioning as an adapter protein that interacts with LC3-II to target aggregates for autophagy-specific degradation [10]. Inhibition of autophagy correlates with increased levels of P62 in mammals, suggesting that steady-state levels of this protein reflect the autophagy status of a cell. Similarly, decreased P62 levels are associated with autophagy activation, as appropriate turnover of P62 is necessary to avoid excessive aggregate clearance [12, 13]. The levels of P62 relative to the levels of LC3 is widely used as a measure of autophagic flux [14].

Beclin1 is a coiled-coil protein that can interact with multiple proteins and is thought to play a role in the control of both autophagic and endocytic fluxes. The involvement of BECLIN1 in autophagy is based on its role in autophagosome maturation. Lately more and more evidence is emerging that the function of BECLIN1 may not be restricted to autophagy but that it can also be involved in processes like phagocytosis and endocytosis. Despite of this, BECLIN1 continues to be considered a marker for early autophagy [reviewed in 15].

Although in general no distinction is made between degeneration of preantral and antral follicles, histological observations suggest that there may be differences between the regulation of preantral and antral follicular degeneration. Spanel-Borowski [16] reported in the bitch two types of atretic patterns in ovarian follicles namely type A in which the oocyte degenerates while granulosa cells remain intact, and type B in which the granulosa cells show signs of extensive degeneration while the oocyte remains initially unaffected. This author further suggested, based on histological analysis, that type A is the predominant form of atresia in preantral follicles, while in antral follicles only type B is observed. In line with these observations, Teerds and Dorrington [17] reported histological differences in atresia of preantral and antral follicles, with oocyte fragmentation, disordered granulosa layer and hypertrophied theca layer being the characteristics of atresia in preantral follicles and massive apoptosis of granulosa cells in the presence of a more or less intact oocyte being characteristic of atresia in antral follicles.

In line with the reports on roles for both autophagy and apoptosis in follicular atresia, the present study addresses the question whether the observed histological differences in preantral and antral follicular atresia are representative of different cell-death pathways. For this purpose, LC3 and P62 are used as markers of autophagy and active, cleaved caspase 3 (cCASP3) [18] is used as a marker of apoptosis, using immunohistochemistry as well as laser capture microdissection (LCM) followed by real-time quantitative reverse transcription polymerase chain reaction (qRT-PCR). Redox homeostasis was probed, using superoxide dismutase 2 (SOD2) immunostaining, as a possible atresia activating mechanism.

Material and Methods

Animals

The Animal Welfare Committee of Wageningen University has approved the animal experiment described in this study (DEC 2004063c). Wistar WU (HsdCpbWU) female rats were bred in the animal facility of Wageningen University. The female rats were weaned at the age of 28 days and

group housed (3 animals per cage). Animals had free access to water and Teklad rat chow (Harlan). The room temperature (20.5-21.5 °C), humidity (55-65%) and light regime (60-80 lux, lights on from 03:00 to 17:00 local daylight saving time) were controlled. Cage enrichment was provided in the form of 10 cm sisal rope. Six female rats were sacrificed at the pro-estrous stage of the estrous cycle at the age of 11 to 14 weeks.

Immunohistochemistry

Rats (n=6) were anesthetized using carbon dioxide and oxygen (flow: 1:2) and killed by decapitation after which ovaries were collected, fixed in 4% phosphate buffered paraformaldehyde and stored at 4 ^{0}C for 24 hours. After fixation, the ovaries were washed in phosphate buffer and embedded in paraffin. Complete ovaries were serial sectioned (5 µm thick paraffin sections; every fifth section was mounted and analyzed as part of a separate study [17]. From the remaining sections of each ovary sections were selected at random (at least 6 sections per ovary for each antibody tested) mounted on super frost plus slides (Menzel, Braunschweig, Germany) and used for immunohistochemical staining. To determine the presence of proteins (LC3, P62, Beclin1, Atg7, cCASP3, and superoxide dismutase 2 (SOD2)) in rat ovaries, immunohistochemistry was performed according to Hoevenaars et al. and Meng et al. [19, 20] with modifications. For each antibody tested, all ovarian sections were stained in one run, in order to be able to compare the immunohistochemical staining among the different animals. Briefly, sections were deparaffinized and rehydrated, after which epitope antigen retrieval in a microwave oven was performed at 96^{0}C (for details see Table 1). Slides were cooled down to room temperature, rinsed with phosphate buffered saline (PBS) 0.01 M, pH7.4 and subsequently endogenous peroxidase activity was blocked with 3% (v/v) hydrogen peroxide in methanol. After rinsing in PBS, sections were incubated with 10% (wt/v) normal goat serum in PBS. Following removal of the goat serum, sections were incubated overnight at 4^{0}C in a humid chamber with the primary antibodies (for details see Table 1) diluted in PBS + 0.05% acetylated bovine serum albumin (BSAc) (Aurion, Wageningen, The Netherlands). Sections were rinsed again and treated with the corresponding secondary biotin-labeled antibody diluted in PBS-BSAc at room temperature (for details see Table 1). The avidin-biotin complex (ABC, Vector Laboratories, Burlingame, CA) was diluted 1:1500 (v/v) or in case of Beclin1

1:1000 (v/v) in PBS-BSAc. Bound antibodies were visualized using 3-3' diaminobenzidine (Immpact DAB, Vector Laboratories) diluted 1:400 (v/v). Sections were counterstained with Mayer's haematoxylin. Control sections were incubated with isotype IgG (Vector Laboratories), instead of the respective primary antibodies, according to the manufactures instructions. The background staining in the controls was negligible.

Follicular nomenclature

Follicles were classified according to Flaws et al. [21] and Slot et al. [22] with minor modifications. Briefly, preantral and antral follicles were identified as healthy when they contained an intact oocyte and an organized granulosa layer with proliferating (mitotic) cells, while the surrounding theca layer had a healthy appearance and did not show any signs of hypertrophy. Atretic preantral follicles were recognized by the presence of a degenerating oocyte, disorganized granulosa cell layer, while the surrounding theca cells showed signs of hypertrophy. Antral follicles were considered to be atretic when more than 5% of the granulosa cells showed morphological signs of apoptosis; the oocyte was either intact and completely surrounded by cumulus granulosa cells, or was partially or no longer surrounded by cumulus granulosa cells and showed signs of resumption of meiosis such as breakdown of the nuclear membrane with or without formation of a pseudo-maturation spindle [23]. As atresia proceeded, the granulosa cells were lost completely and the oocyte degenerated, leaving remnants of the zona pellucida and hypertrophied theca cells. In 4 serial sectioned ovaries the percentage of atretic follicles was determined. In order to prevent double counting of atretic follicles, we counted in three sections per ovary (at a quarter, half and three-quarters of the ovary) all preantral and antral healthy and atretic follicles, independently of the presence of an oocyte, as described previously [20, 21]. Since the counted numbers reflect only part of the total follicle population in an ovary, the mean number of preantral/antral/unknown origin and total atretic follicles was expressed as percentage of the number of non-atretic plus atretic follicles. Primordial and primary follicles were excluded from this counting procedure.

Western blotting

Western blotting was performed Meng et al. [17] with minor modifications. Briefly, ovaries were homogenized in RIPA lysis buffer (50 mM Tris Cl, pH 7.4 / 150 mM NaCl / 1% Nonidet P-40 / 1% sodium deoxycholate / 0.1% SDS) with protease inhibitors (complete Mini-EDTA free, cat no 04693159001, Roche, Mannheim, Germany). The sample was sonicated using the Sonifier Cell Disruptor (Model SLPe, Branson, Eemnes, The Netherlands) and centrifuged for 10 min at 14000 rpm at 4^0C. Protein concentrations were determined using the RC DC Protein Assay Kit II (Bio-Rad, Veenendaal, The Netherlands). SDS-PAGE gels were run using the Mini-Protean Tetra cell system (Bio-Rad). Proteins from the SDS-PAGE gels were transferred onto a 0.20 µm PVDF membrane (Millipore, Amsterdam, The Netherlands). The blot was incubated overnight at 4^0C with the primary antibodies (LC3, diluted 1:200; P62, diluted 1:1000; SOD2, diluted 1:5000; for antibody product information see Table 1) rinsed with PBS-Tween20 (0.1%) followed by incubation for 1 h with IRDye680-conjugated donkey anti-mouse for LC3 and P62 (LI-COR Biosciences, Leusden, The Netherlands) or IRDye800-conjugated donkey anti-rabbit for SOD2 (LI-COR Biosciences) diluted 1:5000 in odyssey blocking buffer (LI-COR Biosciences) at room temperature. Images of the membranes were obtained using the Odyssey infrared imaging system (LI-COR Biosciences).

LCM

To prevent RNA degradation, all the following procedures were conducted under RNase-free conditions. A quick haematoxylin staining protocol followed by LCM was done according to DeCarlo et al [24] with minor modifications. Briefly, sections of ovaries of 6 animals were dehydrated and air-dried for 5 min. The granulosa cells of healthy and atretic antral follicles were captured under 40x magnification (PALM Laser MicroBeam System, P.A.L.M. GmbH, Bernried, Germany in combination with a Zeiss Axioscope microscope, Carl Zeiss, Jena, Germany). Approximately $1x10^4$ granulosa cells per follicle were collected into silicon coated adhesive cap500 caps (Zeiss, Gottingen, Germany). After microdissection, the caps were treated with 20 µl extraction buffer (Picopure RNA Isolation kit, Arcturus, San Diego, CA) and incubated for 30 min at 42^0C. The resulting cell lysates were stored at -80^0C until further use.

RNA isolation and amplification

Total RNA from the cell lysates was extracted using the Picopure RNA Isolation kit (Arcturus) according to the manufacturer's instructions, including on-column DNase treatment (Qiagen, Venlo, The Netherlands). To generate sufficient cDNA samples for qPCR, LCM-derived RNA samples were subjected to mRNA amplification using the Ovation® PicoSL WTA System V2 (Nugen, Leek, the Netherlands) in accordance with the manufacturer's instructions. The cDNA yield was measured by Qubit (ThermoFisher Scientific, Breda, The Netherlands).

qRT-PCR

Quantitative real-time reverse transcription PCR (qRT-PCR) was used to investigate the mRNA expression of the genes *Lc3*, *p62* and *Sod2* in granulosa cells of both healthy and atretic follicles. qRT-PCR reactions were performed with iQ SYBR Green Supermix (Bio-Rad) using the MyIQ single-colour real-time PCR detection system (Bio-Rad). Individual samples were measured in duplicate. A standard curve using serial dilutions of pooled cDNA samples was prepared. A negative control without cDNA template, and a negative control without reverse transcriptase (RT) were included in every assay. Only standard curves with efficiency between 90 and 110% and a correlation coefficient above 0.99 were accepted. Data were normalized against the reference gene ribosomal protein S18 (*Rps18*). Primers were designed using NCBI Primer-Blast (NCBI Web site). Sequences of the used primers were as follows:

Lc3; 5'-CGGGTTGAGGAGACACACAA-3' and 5'-TCTTTGTTCGAAGCTCCGGC-3',

p62; 5'-GCTCATCTTTCCCAACCCCT-3' and 5'-CTGATGGAGCAGAAGCCGAC-3',

Sod2; 5'-GGTGGAGAACCCAAAGGAGAG-3' and 5'-TGATTAGAGCAGGCGGCAAT-3',

Rps18; 5'- TTCAGCACATCCTGCGAGTA-3' and 5'- TTGGTGAGGTCAATGTCTGC-3'.

PCR annealing temperatures of these primers was 60^0C.

Statistical analysis

GraphPad Prism version 5.03 (Graphpad Software, San Diego, USA) was used for statistical analysis

of the qRT-PCR data, with the Student's t test being used to compare mRNA expression in healthy and atretic follicles. The percentages of atretic follicles were analyzed using a one-way ANOVO followed by Tukey post-hoc test. P-values < 0.05 were considered statistically significant.

220

Results

Autophagy and apoptosis in follicular atresia

Preantral follicles

225 The vast majority of follicles present at birth will degenerate before reaching the point of ovulation. The highest incidence of follicular atresia is observed when follicles become dependent on FSH, at the early antral follicle stage. Preantral and preovlatory follicles rarely undergo atresia [3]. It is thus not surprising that the percentage of preantral atretic follicles in the present study was low (Figure 1).

Strong LC3 staining was observed in the granulosa cells of healthy (Figure 2A) and atretic (Figure 2B) 230 preantral follicles in approximately the same stage of development, while staining was faint to absent in theca cells. Clear P62 staining was found in granulosa cells of healthy preantral follicles (Figure 3A), while in granulosa cells of atretic preantal follicles P62 staining was faint to absent (Figure 3B). P62 immunostaining was absent in theca cells. ATG7 immunostaining was absent in granulosa cells of healthy preantral follicles (Figure 4A), but present in granulosa cells of atretic preantral follicles 235 (Figure 4B). Strong ATG7 staining was observed in thecal cells of both of healthy and atretic preantral follicles (Figure 4A,B). There was no difference in BECLIN1 immunostaining apparent between healthy and atretic preantral follicles (Supplemental Figure 1). Immunostaining for cCASP3 was negligible in granulosa and theca cells of healthy (Figure 5A) and atretic preantral follicles (Figure 5B).

240

Antral follicles

The percentage of antral atretic follicles was somewhat higher compared to the percentage of preantral follicles; nevertheless, the origin of most atretic follicles was unknown (Figure 1).

In antral follicles, strong LC3 staining was observed in granulosa cells of healthy (Figure 2C) and

atretic antral follicles (Figure 2D). LC3 staining was faint to absent in the oocytes and theca cells. Clear P62 staining was observed in granulosa cells of healthy antral follicles (Figure 3C), while in granulosa cells of atretic antral follicles P62 immunostaining was moderate to strong (Figure 3D). In theca cells p62 immunostaining was faint to absent. No ATG7 staining was detected in granulosa cells of healthy (Figure 4C) or atretic antral follicles (Figure 4D). Strong ATG7 staining was found in theca cells of both of healthy and atretic antral follicles (Figure 4C,D) as well as in the interstitium in the remnants of atretic follicles (Figure 4). There was no difference in BECLIN1 immunostaining observed between healthy and atretic antral follicles (Supplemental Figure 1). cCASP3 staining was absent in the granulosa and theca cells of healthy antral follicles (Figure 5C), however, many apoptotic cells with cCASP3 positive staining were present in the granulosa layer of atretic antral follicles (Figure 5D).

SOD2 ***and ovarian follicular atresia***

By determining the presence of the antioxidant enzyme SOD2, it was investigated whether mitochondrial accumulation of ROS could play a role in follicular attrition. Moderate to strong SOD2 immunostaining was observed in granulosa cells of healthy preantral (Figure 6A) and antral follicles (Figure 6C). SOD2 staining was faint to absent in granulosa cells of aretic preantral (Figure 6B) as well as antral follicles (Figure 6D). The staining in theca cells of prenatral and antral follicles was faint to moderate and did not undergo changes when follicles underwent atresia (Figure 6). These results suggest that the presence of SOD2 in granulosa cells differed between healthy and atretic follicles.

In order to investigate whether oxidative stress was a cause of follicular atresia, lipid peroxidation was investigated using 4-hydroxynonenal (4-HNE) immunostaining as a marker. No differences were observed in 4-HNE staining between healthy (pre)antral and atretic follicles (Supplemental Figure 2).

Western blotting

To confirm that the antibodies (LC3, P62, SOD2) used in the present study indeed identified the correct proteins in the rat ovary, Western blotting was performed (Supplemental Figure 3). The blot for LC3 showed two clear bands representing LC3 I and LC3 II, two forms that cannot be distinguished

by immunohistochemistry, implicating that the LC3 staining in figure 2 represents total LC3. The blots for P62 and SOD2 showed a single band at the expected size of 62 kDa and 25 kDa, respectively. The validity of the antibody against cCASP3 was tested previously [25, 26].

qRT-PCR

To investigate the gene expression of *Lc3*, *p62* and *Sod2* in granulosa cells of healthy and atretic preantral and antral follicles LCM in combination with qRT-PCR was performed. No difference in *Lc3* and *p62* gene expression was observed between healthy and atretic preantral follicles (Figure 7A) and healthy and atretic antral follicles (Figure 7B). In contrast, *Sod2* mRNA expression was significantly reduced in granulosa cells of atretic preantral and antral follicles compared to healthy follicles at the same stage of development (Figure 7A,B).

Discussion

The present study is to our knowledge the first study that provides evidence that granulosa cell death in preantral and antral follicular atresia are executed by different cell death pathways. Immunohistochemical analysis shows negligible P62 and cCASP3 staining in preantral atretic follicles in combination with the presence of LC3 and ATG7 staining, indicative of autophagy. In contrast, in atretic antral follicles next to LC3, cCASP3 immunostaining is observed while P62 and ATG7 immunostaining are absent, suggesting that granulosa cell death in these follicles is due to apoptosis and that autophagy is not likely to play an important role here. SOD2 immunostaining and mRNA levels are reduced in preantral and antral atretic follicles, suggesting that reduced ROS clearance may play a role in both the induction of preantral and antral follicular atresia.

Although apoptosis has long been considered as the process solely responsible for ovarian follicular demolition [reviewed in 27], previous studies had provided some evidence that this assumption in fact may not be correct. Spanel-Borowski [6, 28] described already in 1981 the presence of a morphological difference between preantral and antral follicular degeneration in the canine ovary.

More than a decade later D'Herde and colleagues [29] identified three different types of granulosa cell death in the avian ovary following starvation-induced follicular atresia, namely apoptotic, autophagic and primary necrotic cell death. Autophagic cell death next to apoptotic cell death is not restricted to vertebrates but has also been identified in ovarian nurse cells during mid and late oogenesis in *Drosophila* virils [30]. Studies in the prepubertal rat ovary, using *in situ* 3'- end labelling of DNA with digoxigenin-deoxy-UTP to detect apoptotic cells, have further made clear that in contrast to antral follicles, apoptosis is minimal in preantral follicles [31]. These observations are fully in line with the negligible cCASP3 immunolabelling in preantral follicles in the present study. At the same time, these studies do not exclude that granulosa cells of preantral follicles are not capable to undergo apoptosis. Withdrawal of diethylstilbestrol stimulation in immature rats results in a significant increase in *in situ* oligoxigenin-dideoxy-UTP labelling of DNA in large preantral follicles [32]. This pathway of preantral granulosa cell death, however, does not seem to be favoured as cell death pathway under normal *in vivo* conditions.

Choi and colleagues [7] have reported a moderate to strong immunostaining of the authophagy marker LC3 in granulosa cells of healthy primordial up to late antral follicles in immature rats treated with equine chorionic gonadotropin. Significant LC3 staining was further observed in atretic antral follicles, while co-localization of LC3 and cCASP3 immunostaining was observed in antral follicles, but not in preantral follicles [7]. Additional evidence for the assumption that apoptosis is not the only death pathway active in the ovary comes from studies in which adult female mice are exposed to cigarette smoke. Exposure for 8 weeks results in a decrease in preantral follicle numbers without a concomitant increase in apoptosis, as no change in the staining of the apoptosis markers cCASP3 and TUNEL is observed [33]. At the same time the ovarian levels of the autophagy marker LC3 and the autophagy homeostasis associated protein BECLIN1 are increased, suggesting that cigarette smoke induces degenration of preantral follicles by activation of the autophagy cascade [34]. By using P62 and AGT7 next to LC3 as markers for autophagy, the results of the present study add to these observations that the default pathway of degeneration in preantral follicles is through autophagy, and that activation of this pathway occurs under normal physiological conditions, independent of the presence of xenotoxic

stressors.

Another early marker frequently used to identify autophagy is BECLIN1. The function of BECLIN1 in cell survival and cell death is however complex, as BECLIN1 appears to be involved not only in the regulation of autophagy but also of apoptosis. BECLIN1 being a BH3-only protein can form a complex with BCL2, BCL-XL, BCL-W or MCL1. The BCL22/BCL-XL-BECLIN1 interaction does not inhibit the anti-apoptotic function of BCL2 but does inhibit BECLIN1 mediated induction of autophagy; the BCL2 – BECLIN1 complex needs to be dissociated in order for BECLIN1 to induce autophagy. Dissociation can among others be achieved through JNK-mediated phosphorylation of BCL2 and death-associated protein kinase (DAPK)-mediated phosphorylation of BECLIN1 [35,36]. In line with this, we did not observe any difference in BECLIN1 staining between preantral and antral atretic follicles, neither was there a difference in BECLIN1 immunostaining between healthy and atretic follicles. We therefore are the opinion that in the normal adult ray ovary BECLIN1 does not seem to be an appropriate marker to discriminate between autophagy and apoptosis.

One of the processes that is suggested to play a role in smoke induced activation of the autophagic cascade is oxidative stress. Cigarette smoke exposure leads to an increase in ovarian expression of HSP25, a small heath shock protein that is up-regulated under conditions of oxidative stress, while SOD2 expression is decreased, suggestive of loss of antioxidant activity [33]. In the present study, we observe a strong reduction in both SOD2 immunostaining and granulosa cell *Sod2* mRNA content in preantral as well as antral atretic follicles. Although this may implicate that both autophagy in preantral follicles and apoptosis in antral follicles may be triggered by a loss in mitochondrial antioxidant capacity in granulosa cells, we were unable to confirm the presence of oxidative stress in atretic (pre)antral follicles using 4-HNE a marker for lipid peroxidation. To what extend oxidative stress plays a role in autophagy induced preantral and apoptosis induced antral follicular atresia remains to be investigated.

The next question that arises is, which pathway is involved in activation of granulosa cell autophagy. It

has been shown that cigarette smoke exposure of rats leads to activation of AMP activated protein kinase alpha 1 (AMPK-α1) and AMPK-α2 in the ovary, while at the same time expression of the prosurvival factors AKT and mammalian target of rapamycin complex 1 (mTORC1) is decreased [37]. AMPK is an important regulator of metabolism, an inhibitor of the mTORC1 complex and a direct activator of autophagy [38, 39]. Its activity is sensitive to ROS [35]. The data from Furlong *et al*. [37] suggest that cigarette smoke induced oxidative stress activates AMPK, leading to activation of autophagy and inhibition of mTORC1. Support for this hypothesis comes from a study by Choi et al, who demonstrated that AKT-mediated activation of mTORC1 suppresses granulosa cell autophagy during follicular development *in vivo* as well as *in vitro* [41]. The reduced *Sod2* mRNA expression in granulosa cells of preantral follicles suggests that this pathway may also be involved in preantral follicular atresia under physiological conditions, although this will need confirmation by additional experiments. Lack of activation of the NRF2 antioxidant response pathway by decreased P62 levels may occur in preantral follicle atresia [42] but does not provide an explanation for antral follicle atresia, where P62 is not affected.

We did not observe a difference in *P62* mRNA expression in granulosa cells from healthy and atretic preantral follicles, despite the obvious differences in immunostaining. Furlong et al were also unable to detect any differences in *P62* mRNA expression and protein content between healthy and autophagic granulosa cells [37]. These authors hypothesised that the absence of a change in *P62* gene expression may be due to the large variability between control and treated groups. This does not seem to be the case in our analysis. It is well established that a major part of the regulation of P62 occurs post-translationally [43]. Indeed, a change in P62 protein levels, without a difference in *P62* mRNA has also been seen in other studies (e.g. [44,45]). Pursiheimo and colleagues demonstrated for instance that hypoxia-induced autophagy in cancer cells led to a down regulation in P62 protein content, while mRNA levels were not affected [44]. The opposite has also been reported. In a recent study, Ning and colleagues showed under *in vitro* conditions that exposure of THP-1-derived macrophages to oxidized LDL resulted in an increase in P62 protein content, while at the same time *P62* mRNA expression was down regulated, thus inhibiting autophagy [46]. These studies further stress that in order to investigate

the involvement of P62 in autophagy, protein expression needs to be included.

In contrast to preantral follicular atresia, it is believed generally that antral follicular atresia and thus granulosa cell apoptosis is triggered by insufficient FSH levels or reduced numbers of FSH receptors [47]. FSH is thought to rescue granulosa cells of antral follicles from apoptosis via activation of the phosphatidylinositol 3-kinase (PI3K)–AKT signal transduction pathway. Activation of PI3K-AKT via binding of FSH to its receptor leads to phosphorylation of the forkhead box O (FOXO) subfamily of forkhead transcription factors which influences, among other processes, survival of granulosa cells. In the presence of insufficient FSH signalling, FOXOs are dephosphorylated and translocate to the nucleus, resulting in enhanced transcription of pro-apoptotic factors [reviewed in [41]]. These observations implicate a role for the AKT signalling pathway not only in autophagy but also in apoptosis induced granulosa cell death. By influencing AKT though different pathways granulosa cells will either undergo autophagy (in FSH-independent preantral follicles) or apoptosis (in FSH-dependent antral follicles).

In conclusion, the results of the present study show that antral follicular atresia is initiated by massive granulosa cell apoptosis, while preantral follicles atresia occurs mainly via enhanced granulosa cell autophagy.

Acknowledgements

The authors would like to thank Eddy Rijntjes, Hans Swarts and Inge van der Stelt for their assistance.

Reference

1. McGee EA, Hsueh AJ. Initial and cyclic recruitment of ovarian follicles. Endocr Rev 2000; 21:200-214.
2. Hsueh AJ, Kawamura K, Cheng Y, Fauser BC. Intraovarian control of early folliculogenesis. Endocr Rev 2015; 36:1-24.
3. Chun S-Y, Eisenhauer KM, Minami S, Billig H, Perlas E, Hsueh AJW. Hormonal regulation of apoptosis in early antral follicels: Follicles-stimulating hormone as a major survival factor. Endocrinology 1996; 17:1447-1456.
4. Kaipia A, Hsueh AJ. Regulation of ovarian follicle atresia. Annu Rev Physiol 1997; 59:349-363.
5. Hulas-Stasiak M, Gawron A. Follicular atresia in the prepubertal spiny mouse (Acomys cahirinus) ovary. Apoptosis 2011; 16:967-975.
6. Duerrschmidt N, Zabirnyk O, Nowicki M, Ricken A, Hmeidan FA, Blumenauer V, Borlak J, Spanel-Borowski K. Lectin-like oxidized low-density lipoprotein receptor-1-mediated autophagy in human granulosa cells as an alternative of programmed cell death. Endocrinology 2006; 147:3851-3860.
7. Choi JY, Jo MW, Lee EY, Yoon BK, Choi DS. The role of autophagy in follicular development and atresia in rat granulosa cells. Fertil Steril 2010; 93:2532-2537.
8. Loos B, Engelbrecht AM, Lockshin RA, Klionsky DJ, Zakeri Z. The variability of autophagy and cell death susceptibility: Unanswered questions. Autophagy 2013; 9:1270-1285.
9. Wirawan E, Vanden Berghe T, Lippens S, Agostinis P, Vandenabeele P. Autophagy: for better or for worse. Cell Res 2012; 22:43-61.
10. Klionsky DJ, Schulman BA. Dynamic regulation of macroautophagy by distinctive ubiquitin-like proteins. Nat Struct Mol Biol 2014; 21:336-345.
11. Xiong J. Agt7 in development and disease. Panacea or Pandora's Box? Protein Cell 2015; 6:722-734.
12. Klionsky DJ, Abdalla FC, Abeliovich H, Abraham RT, Acevedo-Arozena A, Adeli K, Agholme L, Agnello M, Agostinis P, Aguirre-Ghiso JA, Ahn HJ, Ait-Mohamed O, et al.

Guidelines for the use and interpretation of assays for monitoring autophagy. Autophagy 2012; 8:445-544.

13. Klionsky DJ, Abdelmohsen K, Abe A, Abedin MJ, Abeliovich H, Arozena AA, Adachi H, Adams CM, Adams PD, Adeli K, Adhihetty PJ, Adler SG, et al. Guidelines for the use and interpretation of assays for monitoring autophagy (3rd edition). Autophagy 2016; 12:1-222.
14. Mizushima N, Yoshimori T. How to interpret LC3 immunoblotting. Autophagy 2007; 3:542-545.
15. Salminen A, Kaarniranta K, Kauppinen A. Beclin 1 interactome controls the crosstalk between apoptosis, autophagy and inflammasome activation: Impact n the aging process. Ageing Res Rev 2013; 12:520-534.
16. Spanel-Borowski K. Follicle stages and follicular atresia. In: Atlas of the Mammalian Ovary. Springer-Verlag Berlin Heidelberg 2012;9-22
17. Teerds KJ, Dorrington JH. Immunohistochemical localization of 3 beta-hydroxysteroid dehydrogenase in the rat ovary during follicular development and atresia. Biol Reprod 1993; 49:989-996.
18. Matikainen T, Perez GI, Zheng TS, Kluzak TR, Rueda BR, Flavell RA, Tilly JL. Caspase-3 gene knockout defines cell lineage specificity for programmed cell death signaling in the ovary. Endocrinology 2001; 142:2468-2480.
19. Hoevenaars FPM, Keijer J, Herreman L, Palm I, Hegeman MA, Swarts HJM, van Schothorst EM. Adipose tissue metabolism and inflammation are differently affected by weight loss in obese mice due to either a high-fat diet restriction or change to a low-fat diet. Genes Nutr 2014; 9.
20. Meng L, Rijntjes E, Swarts H, Bunschoten A, van der Stelt I, Keijer J, Teerds K. Dietary-induced chronic hypothyroidism negatively affects rat follicular development and ovulation rate and is associated with oxidative stress. Biol Reprod 2016; 94:1-11.
21. Flaws JA, Abbud R, Mann RJ, Nilson JH, Hirshfield AN. Chronically elevated luteinizing hormone depletes primordial follicles in the mouse ovary. Biol Reprod 1997; 57:1233-1237.
22. Slot KA, Kastelijn J, Bachelot A, Kelly PA, Binart N, Teerds KJ. Reduced recruitment and

survivial of primordial and growing follicles in GH receptor deficient mice. Reproduction 2006; 131:525-532.

23. Osman P. Rate and course of atresia during follicular development in the adult cyclic rat. J Reprod Fertil 1985; 73:261-270.

24. DeCarlo KEA, Dadzie OE, Mahaligam M. Laser capture microdisection: methods and protocols. In: Murray GI (ed). Laser capture microdisection: methods and applications. Meth Mol Biol 2011; 755:1-15.

25. Boada-Romero E, Serramito-Gomez I, Sacristan MP, Boone DL, Xavier RJ, Pimentel-Muinos FX. The T300A Crohn's disease risk polymorphism impairs function of the WD40 domain of ATG16L1. Nat Commun 2016; 7.

26. Fan L, Peng G, Sahgal N, Fazli L, Gleave M, Zhang Y, Hussain A, Qi J. Regulation of c-Myc expression by the histone demethylase JMJD1A is essential for prostate cancer cell growth and survival. Oncogene 2016; 35:2441-2452.

27. Kaipa A, Hsueh AJW. Regulation of ovarian follicle atresia. Annu Rev Physiol 1997; 59:349-363.

28. Spanel-Borowski K. Morphological investigations on follicular atresia in Canine ovaries. Cell Tissue Res 1981; 214:155-168.

29. D'Herde K, De Prest B, Roels F. Subtypes of active cell death in the granulosa of ovarian atretic follicles in the quail (*Coturnix coturnix japonica*). Reprod Nutr Dev 1996; 36:175-189.

30. Velentzas AD, Nezis IP, Stavopodis DJ, Papassideri IS, Margaritis LH. Apoptosis and autophagy function cooperatively for the efficacius execution of programmed nurse cell death during *Drosophila virilis* oogenesis. Autophagy 2007; 3:130-132.

31. McGee E, Spears N, Minami S, Hsu SY, Chun SY, Billig H, Hsueh AJW. Preantral ovarian follicles in serum-free culture: Suppression of apoptosis after activation of the cyclic guanosine 3',5'-monophosphate pathway and stimulation of growth and differentiation by follicle-stimulating hormone. Endocrinology 1997; 138:2417-2424.

32. Billig H, Furuta I, Hsueh AJW. Estrogens Inhibit and androgens enhance ovarian granulosa-cell apoptosis. Endocrinology 1993; 133:2204-2212.

33. Gannon AM, Stampfli MR, Foster WG. Cigarette smoke exposure leads to follicle loss via an alternative ovarian cell death pathway in a mouse model. Toxicol Sci 2012; 125:274-284.

34. Gannon AM, Stampfli MR, Foster WG. Cigarette smoke exposure elicits increased autophagy and dysregulation of mitochondrial dynamics in murine granulosa cells. Biol Reprod 2013; 88:1-11.

35. Grody C, He Y-W. The crosstalk between autophagy and apoptosis: where does this lead? Protein Cell 2012; 3:17-27.

36. Kang R, Zeh HJ, Lotze MT, Tang D. The Beclin 1 network regulates autophagy and apoptosis. Cell Death Diff 2011; 18:571-580.

37. Furlong HC, Stampfli MR, Gannon AM, Foster WG. Cigarette smoke exposure triggers the autophagic cascade via activation of the AMPK pathway in mice. Biol Reprod 2015; 93:1-10.

38. Kim J, Kundu M, Viollet B, Guan KL. AMPK and mTOR regulate autophagy through direct phosphorylation of Ulk1. Nat Cell Biol 2011; 13:132-U171.

39. Egan DF, Shackelford DB, Mihaylova MM, Gelino S, Kohnz RA, Mair W, Vasquez DS, Joshi A, Gwinn DM, Taylor R, Asara JM, Fitzpatrick J, et al. Phosphorylation of ULK1 (hATG1) by AMP-activated protein kinase connects energy sensing to Mitophagy. Science 2011; 331:456-461.

40. Emerling BM, Weinberg F, Snyder C, Burgess Z, Mutlu GM, Viollet B, Budinger GRS, Chandel NS. Hypoxic activation of AMPK is dependent on mitochondrial ROS but independent of an increase in AMP/ATP ratio. Free Radical Bio Med 2009; 46:1386-1391.

41. Choi J, Jo M, Lee E, Choi D. AKT is involved in granulosa cell autophagy regulation via mTOR signaling during rat follicular development and atresia. Reproduction 2014; 147:73-80.

42. Kumatzu M, Kurokawa H, Waguri S, Tagichi K, Kobayashi A, Ichimura Y, Sou YS, Ueno I, Sakamoto A, Tong KI, Kim M, Nishito Y et al. The selective autophagy substrate p62 activates the stress responsive transcription factor *Nrf2* through inactivation of *Keap1*. Nat Cell Biol 2010; 12:213-223.

43. Lim J, Lachenmayer ML, Wu S, Kundu M, Wang R, Komatsu M, Oh YJ, Zhao Y, Yue Z. Proteotoxic stress induces phosphorylation of p62/SQSTM1 by ULK1 to regulate selective

autophagic clearance of protein aggregates. PLoS Genet 2015; 11(2):e1004987.

44. Pursiheimo JP, Rantanen K, Heikkinen PT, Johansen T, Jaakkola PM. Hypoxia-activated autophagy accelerates degradation of SQSTM1/p62. Oncogene 2009; 28:334-344.

45. Narendra DP, Kane LA, Hauser DN, Fearnley IM, Youle RJ. p62/SQSTM1 is required for Parkin-induced mitochondrial clustering but not mitophagy; VDAC1 is dispensable for both. Autophagy 2010; 6:1090-1106.

46. Ning H, Liu D, Yu X, Guan X. Oxidized low-density lipoprotein-induced p62/SQSTM1 accumulation in THP-1 derived macrophages promotes IL-18 secretion and cell death. Exp Ther Med 2017; 14:5417-5423.

47. Matsuda F, Inoue N, Manabe N, Ohkura S. Follicular growth and atresia in mammalian ovaries: regulation by survival and death of granulosa cells. J Reprod Dev 2012; 58:44-50.

Figure legends

Figure 1 – Percentage of atretic preantral and antral follicles, atretic follicles of unknown origin and total percentage of atretic follicles. Data were analysed by one-way ANOVA followed by Tukey post-hoc test. Values are expressed as mean $\pm$ SD, n=4; (a) significantly different from preantral follicles, (b) significantly different from antral follicles, $P < 0.05$.

Figure 2 – Representative LC3 staining (brown) of the adult rat ovary. (A) Healthy preantral follicle with clear LC3 staining in granulosa cells; (B) Atretic preantral follicle with clear LC3 staining in granulosa cell, the disorganized granulosa layer is indicated by a surrounding dashed line and hypertrophied theca cells are indicated by a dotted two-sided arrow; (C) Healthy early antral follicle with clear LC3 staining in granulosa cells; (D) Atretic early antral follicle with clear LC3 staining in granulosa cells. Granulosa cells are indicated by asterisks, theca cells by arrowheads and oocytes by arrows. Scale bars represent 50 μm.

Figure 3 – Representative SQSTM1/P62 immunostaining (brown) of an adult rat ovary. (A) Healthy preantral follicle with clear P62 staining in granulosa cells; (B) Atretic preantral follicle with faint to absent P62 staining in granulosa cells, the disorganized granulosa layer is indicated by a surrounding dashed line and hypertrophied theca cells are indicated by dotted two-sided arrows; (C) Healthy early antral follicle with clear P62 staining in granulosa cells; (D) Atretic early antral follicle with moderate to clear P62 staining in granulosa cells. Granulosa cells are indicated by asterisks, theca cells by arrowheads and oocytes by arrows. Scale bars represent 50 μm.

Figure 4 – Representative AGT7 immunostaining (brown) in the adult rat ovary. (A) In healthy preantral follicles AGT7 immunostaining is absent in granulosa cells; (B) Atretic preantral follicle with ATG7 staining in granulosa cells, the disorganized granulosa layer is indicated by a surrounding dashed line and hypertrophied theca cells are indicated by dotted two-sided arrows; (C) Healthy early antral follicle and (D) atretic antral follicle in which no detectable AGT7 immunostainig is observed. Theca cells always stain positive for the presence of ATG7. Granulosa cells are indicated by

asterisks, theca cells by arrowheads and oocytes by arrows. Scale bars represent 50 μm.

Figure 5 – Representative active, cleaved caspase 3 (cCASP3) immunostaining (brown) of an adult rat ovary. (A) Healthy preantral follicle with no cCASp3 staining in granulosa cells; (B) Atretic preantral follicle with no cCASp3 staining in granulosa cells, the disorganized granulosa cells is indicated by a surrounding dashed line and hypertrophied theca cells are indicated by a dotted two sided arrow; (C) Healthy large antral follicle, note the absence of cCASP3 staining in granulosa cells (detail shown in insert); (D) Atretic large antral follicles with numerous granulosa cell derived apoptotic bodies adjacent to and within the antrum that stain positively for the presence of cCASP3 (detail shown in insert). Granulosa cells are indicated by asterisks, theca cells by arrowheads and oocytes by arrows. Scale bars represent 50 μm.

Figure 6 – Representative SOD2 immunostaining (brown) in an adult rat ovary. (A) Healthy late preantral follicle with moderate to strong SOD2 staining in granulosa cells; (B) Atretic preantral follicle with faint to absent SOD2 staining in granulosa cells, the disorganized granulosa cells are indicated by a surrounding dashed line and hypertrophied theca cells are indicated by a dotted two sided arrow; (C) Healthy antral follicle with clear SOD2 staining in the granulosa cells (detail shown in insert); (D) Atretic antral follicle with faint to absent SOD2 staining in the granulosa cells (detail shown in insert). Granulosa cells are indicated by asterisks, theca cells by arrowheads and oocytes by arrows. Scale bars represent 50 μm.

Figure 7 – Gene expression in granulosa cells of healthy (open circles, n=6) and atretic follicles (filled squares, n=6) as measured by qRT-PCR. Differences in gene expression are expressed as ratio of mRNA levels in atretic follicles over healthy follicles, with no change indicated as 1/-1 or -1. (A) Healthy and atretic preantral follicles; (B) Healthy and atretic antral follicles; *Lc3,* microtubule-associated protein 1 light chain 3; *p62, Sqstm1, sequestosome 1*; *Sod2*, superoxide dismutase 2; ****, $p<0.0001$

Supplemental Figure 1 - Representative Beclin 1 staining (brown) of the adult rat ovary. (A) Healthy preantral follicle; (B) Atretic preantral follicle; (C) Healthy early antral follicle; (D) Atretic early antral follicle. Beclin 1 staining is present in the granulosa cells of healthy and atretic (pre)antral follicles, and to a lesser extent in the theca cells. No difference in immunostaining between healthy and atretic was observed. Granulosa cells are indicated by asterisks, theca cells by arrowheads and oocytes by arrows. Scale bars represent 50 μm.

Supplemental Figure 2 - Representative 4-HNE staining of the adult rat ovary; 4-HNE staining is negligible in preantral (A) and antral (B) atretic follicles. Granulosa cells are indicated by asterisks, theca cells by arrowheads and oocytes by arrows. Scale bars represent 50 μm.

Supplemental Figure 3 – Western blot representing the presence of LC3, P62 and SOD2 in homogenates of rat ovaries after separation by SDS-polyacrylamide gel electrophoresis. The specific band at the expected size is indicated by an arrow.

Table 1 - Antibodies used for immunohistochemistry.

Primary antibody	Antigen retrieval buffer (10 mM)	Primary antibody dilution	Secondary antibody dilution	Source	Lot Number
LC3	Tris/EDTA pH 9 (15 min)	1:100	Goat anti-mouse, 1:200	Nano Tools (0231-100/LC3-5 F10), Teningen, Germany	0231s0302
Beclin1	Sodium citrate pH 6 (10 min)	1:5000	Goat-anti-rabbit 1:400	Abcam plc (ab62472), Cambridge, UK	
Atg7	Sodium citrate pH 6 (10 min)	1:100	Goat-anti-rabbit 1:200	Proteintech (10088-2-AP), Fisherscientific, Manchster, UK	00051656
SQSTM1/ p62	Sodium citrate pH 6 (10 min)	1:500	Goat anti-mouse, 1:400	Abcam plc (ab56416), Cambridge, UK	GR108093-1
cCASP3	Tris/EDTA pH 9 (10 min)	1:3000	Goat anti-rabbit, 1:400	Cell signalling (CST9661S), Bioke, The Netherlands	42
SOD2	Sodium Citrate pH 6 (10 min)	1:1000	Goat anti-rabbit, 1:400	Abcam plc (ab13533) Cambridge, UK	GR67500-4

All secondary antibodies were obtained from Vector Laboratories (Vector, Burlingame, CA, USA).

Figure 1

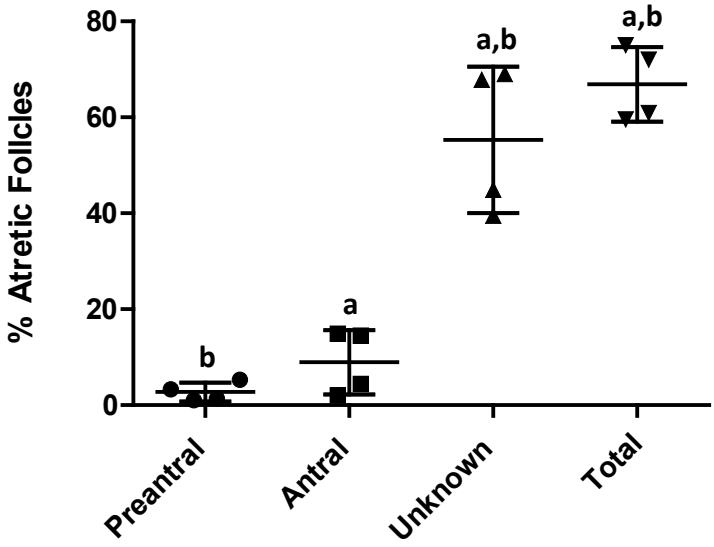
% Atretic Follcles
80
60
40
20
0
b
a
a,b
a,b
Preantral
Antral
Unknown
Total

Figure 2

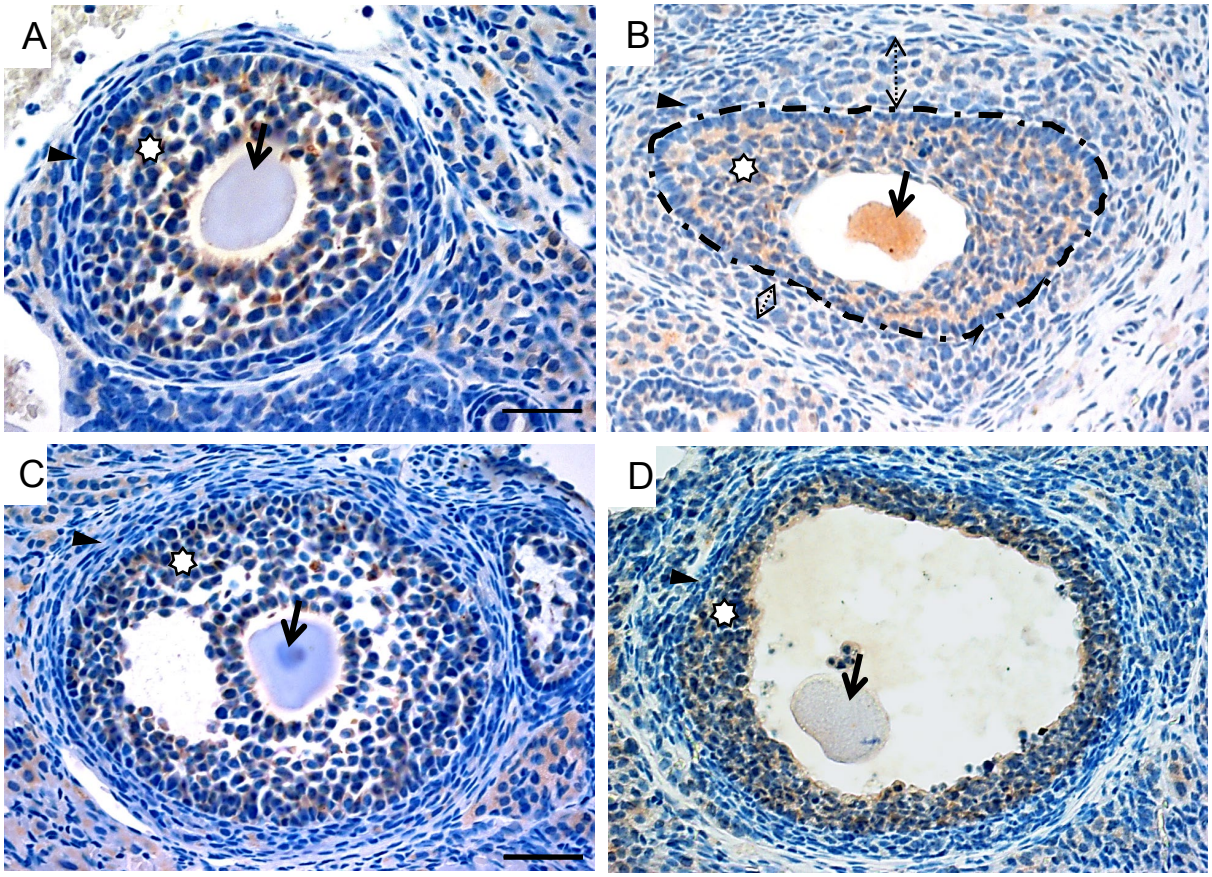

Figure 3

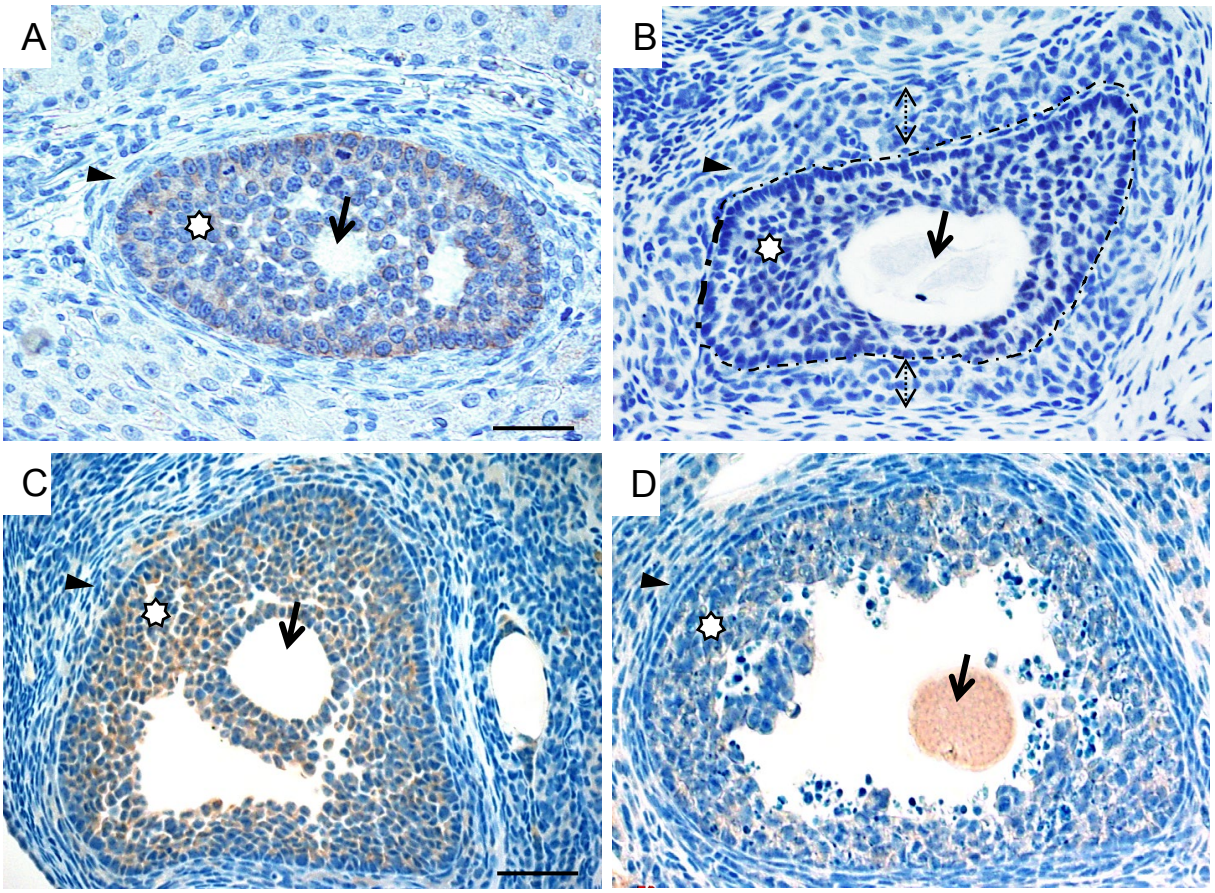

Figure 4

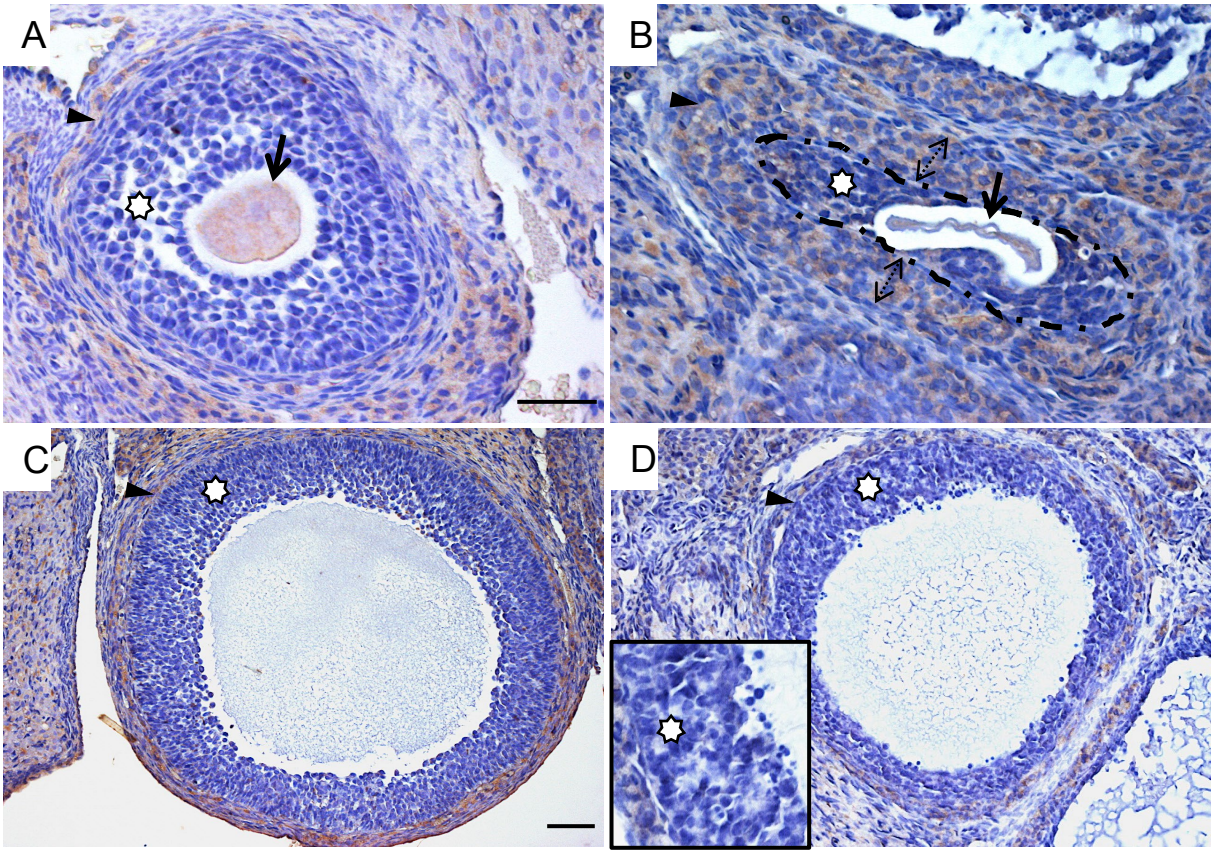

Figure 5

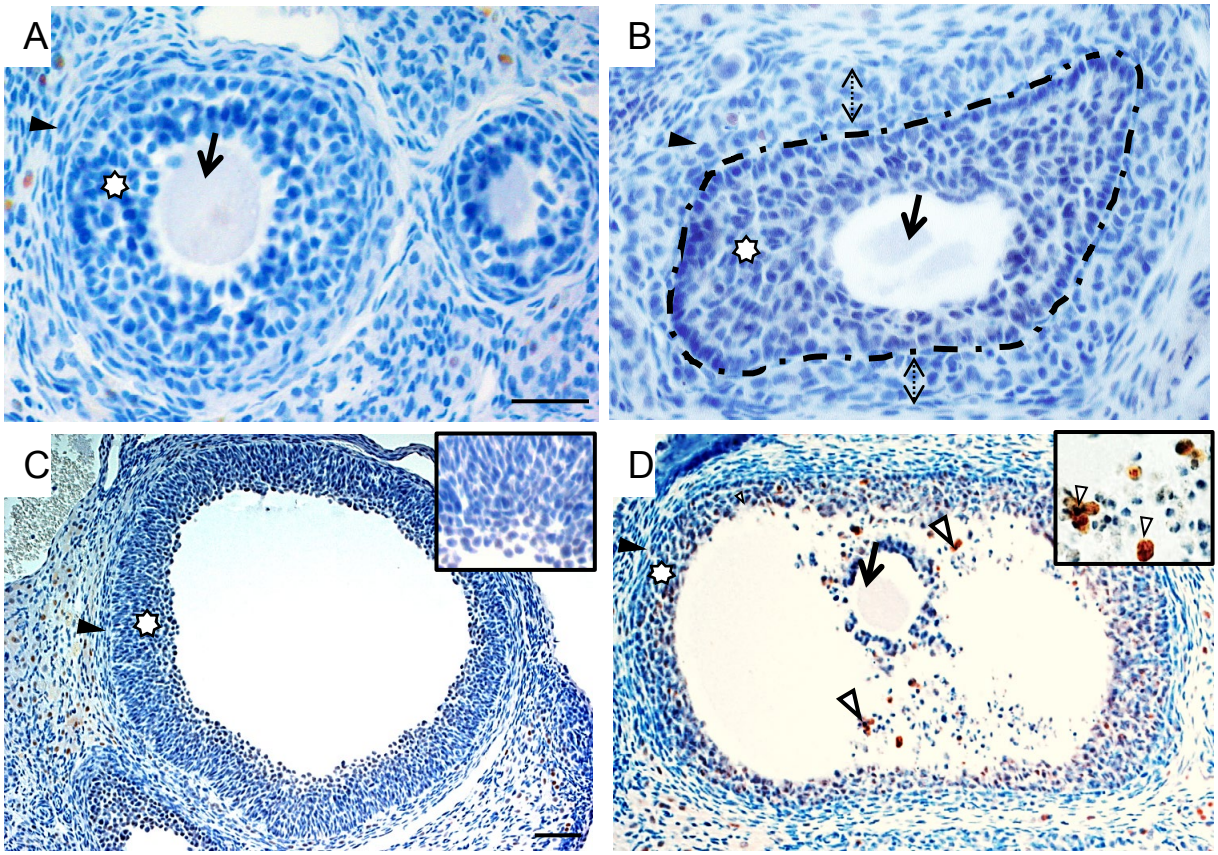

Figure 6

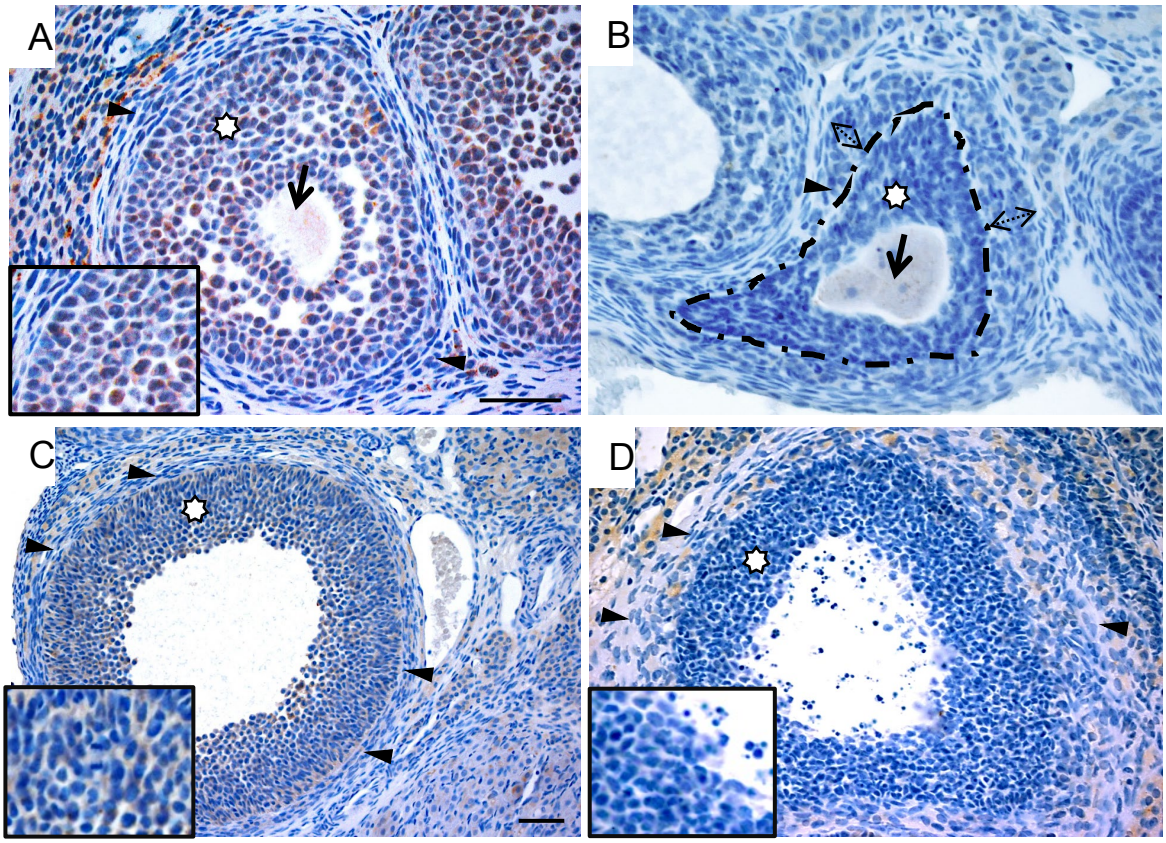

Figure 7

A
Preantral follicles

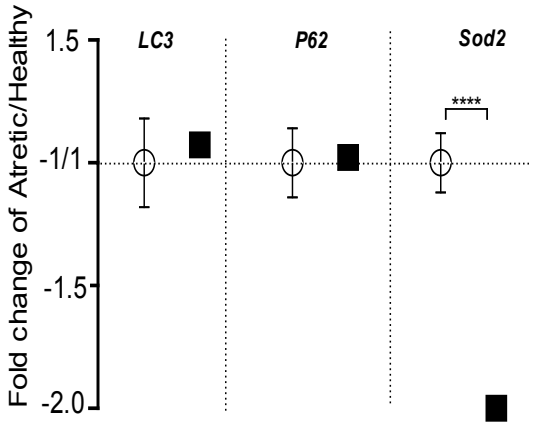

B
Antral follicles